University Library

A gateway to Melbourne's research publications

Minerva Access is the Institutional Repository of The University of Melbourne

Author/s:
Mynard, JP;Wasserman, BA;Steinman, DA

Title:
Errors in the estimation of wall shear stress by maximum Doppler velocity

Date:
2013-04-01

Citation:
Mynard, J. P., Wasserman, B. A. & Steinman, D. A. (2013). Errors in the estimation of wall shear stress by maximum Doppler velocity. Atherosclerosis, 227 (2), pp.259-266. https://doi.org/10.1016/j.atherosclerosis.2013.01.026.

Persistent Link:
https://hdl.handle.net/11343/58860

Errors in the estimation of wall shear stress by maximum Doppler velocity

Jonathan P. Mynard[a], Bruce A. Wasserman[b], David A. Steinman[a]

[a] Biomedical Simulation Laboratory, Department of Mechanical and Industrial Engineering, University of Toronto, 5 King's College Rd, Toronto, Ontario, M5S 3G8, Canada

[b] The Russell H. Morgan Department of Radiology and Radiological Sciences, The Johns Hopkins University School of Medicine, 601 North Caroline St, Baltimore, MD 21287, USA

Corresponding Author:

David A. Steinman

Phone: +1 416 978 7781

Fax: +1 416 978 7773

steinman@mie.utoronto.ca

Other author email addresses

JPM: jmynard@mie.utoronto.ca

BAW: bwasser@jhmi.edu

Abstract

Objective. Wall shear stress (WSS) is an important parameter with links to vascular (dys)function. Difficult to measure directly, WSS is often inferred from maximum spectral Doppler velocity (V_{max}) by assuming fully-developed flow, which is valid only if the vessel is long and straight. Motivated by evidence that even slight/local curvatures in the nominally straight common carotid artery (CCA) prevent flow from fully developing, we investigated the effects of velocity profile skewing on V_{max}-derived WSS.

Methods. Velocity profiles, representing different degrees of skewing, were extracted from the CCA of image-based computational fluid dynamics (CFD) simulations carried out as part of the VALIDATE study. Maximum velocities were calculated from idealized sample volumes and used to estimate WSS via fully-developed (Poiseuille or Womersley) velocity profiles, for comparison with the actual (i.e. CFD-derived) WSS.

Results. For cycle-averaged WSS, mild velocity profile skewing caused ±25% errors by assuming Poiseuille or Womersley profiles, while severe skewing caused a median error of 30% (maximum 55%). Peak systolic WSS was underestimated by ~50% irrespective of skewing with Poiseuille; using a Womersley profile removed this bias, but ±30% errors remained. Errors were greatest in late systole, when skewing was most pronounced. Skewing also introduced large circumferential WSS variations: ±60%, and up to ±100%, of the circumferentially averaged value.

Conclusion. V_{max}-derived WSS may be prone to substantial variable errors related to velocity profile skewing, and cannot detect possibly large circumferential WSS variations. Caution should be exercised when making assumptions about velocity profile shape to calculate WSS, even in vessels usually considered long and straight.

Keywords: Doppler ultrasound, wall shear stress, atherosclerosis, computational fluid dynamics, common carotid artery, brachial artery, femoral artery

1. Introduction

Wall shear stress (WSS) represents the shearing force exerted by blood flow on vascular endothelial cells, and is widely thought to play a key role in vascular reactivity [1], wall thickening [2] and atherosclerosis [3, 4]. Although direct and precise measurement of WSS metrics (such as mean, maximum, and circumferential variation of WSS) in the clinic would therefore be highly desirable, this goal has not yet been achieved, primarily due to resolution limits of current imaging modalities. For example, WSS is non-linearly underestimated by magnetic resonance imaging (MRI) [5], while accurate measurement of velocities near the moving arterial wall via Doppler ultrasound is extremely difficult [6].

A popular alternative to direct measurement of near-wall velocities is to estimate WSS from an assumed velocity profile. A common approach in Doppler studies has been to assume a parabolic (i.e. Poiseuille) profile and calculate WSS via the resulting formula $4\mu V_{max}/D$; where μ is blood viscosity, D is the vessel diameter and V_{max} is the maximum instantaneous velocity [1, 2, 7-10]. This neglects the possible blunting of the systolic velocity profile caused by flow pulsatility, so a number of investigators have instead used a Womersley profile to estimate WSS [11, 12].

Underpinning the calculation of WSS from parabolic or Womersley profiles is the assumption that the velocity profile is axisymmetric and fully-developed (with V_{max} lying on the centreline), thus limiting the measurement to vessels that are long and straight. However, vessels typically assumed to be long and straight (e.g. brachial, femoral and common carotid arteries (CCA)) may often harbor undeveloped or skewed velocity profiles owing to mild curvature [13-15]. Velocity profile skewing has three potential consequences for estimating WSS via Doppler ultrasound. First, a small, centrally-located sample volume may not detect true V_{max}. Second, the departure from ideal Poiseuille or Womersley profiles may lead to errors in calculated WSS.

Finally, velocity profile skewing is likely to be associated with circumferential WSS variations, which cannot be captured by V_{max}-based calculations.

The aim of this study was to determine the likely errors in Doppler WSS measurement arising from these three issues, using anatomically realistic, image-based computational fluid dynamics (CFD) models of the CCA. This study extends our recent work investigating the accuracy of volume flow variables derived from Doppler V_{max} [16].

2. Methods

2.1 Study Participants and Image Acquisition

Eighteen subjects (age range, 37-84 years; mean±SD, 58±15) without carotid stenosis were selected from a subset of the VALIDATE study (Vascular Aging – The Link That Bridges Age To Atherosclerosis) representing 'normal vascular aging', consisting of subjects recruited from the Baltimore Longitudinal Study of Aging [17]. The study was approved by institutional review boards and subjects provided written informed consent. Contrast-enhanced magnetic resonance angiograms (CEMRA) and phase contrast magnetic resonance imaging (PCMRI) sequences were acquired as described by Hoi et al [18].

2.2 Computational Fluid Dynamics (CFD)

Model geometry was obtained by segmenting the right carotid bifurcation from CEMRA images using the Vascular Modelling ToolKit (www.vmtk.org), with the CCA segmented to its thoracic origin, and CFD was performed with a validated solver, as in [16]. Second-order tetrahedral volume meshes were generated with a nominal edge length of 0.25 mm, previously demonstrated by our group to adequately resolve carotid WSS distributions [19]. Inlet and outlet pulsatile flow rates were obtained from PCMRI images and prescribed at the CCA and internal carotid artery (ICA) boundaries, assuming fully-developed axial Womersley velocity profiles, having adjusted ICA flow by the factor CCA/(ICA+ECA) at each time point to ensure instantaneous flow

conservation. A traction-free boundary condition was used for the external carotid artery (ECA), vessel walls were assumed to be rigid and blood viscosity and blood density were 0.035 cm^2/s and 1.06 g/cm^3 respectively.

2.3 Data analysis

The data analysis procedure was similar to that described in [16]. Briefly, two-dimensional axial velocity profiles were extracted from CFD data at 3, 7 and 11 maximally-inscribed sphere radii proximal to the bifurcation, i.e. 1.2±0.2, 2.2±0.4 and 3.3±0.5 cm from the bifurcation apex respectively, consistent with the reported range of 1-3 cm (see [16]). The degree of velocity profile skewing in the common carotid artery was classified by analysis of the high velocity region (HVR) [13], a contiguous area of pixels containing the highest velocities and covering 25% of the lumen area. Using an automated algorithm [13], the shape of the HVR boundary was used to classify the cycle-averaged velocity profile as Type I (axisymmetric), Type II (skewed) or Type III (highly skewed, or crescent-shaped) (Fig. 1).

From the total data set, six Type I, six Type II and twelve Type III profiles were selected, with a greater number of Type III profiles selected because these were expected to exhibit the greatest departure from fully-developed axisymmetric flow. As in [16], if multiple profiles from the three slice locations in a given subject had the same type, only one of these was included in the analysis (selected randomly). Note that Ford et al's analysis of PC-MRI data of the undiseased CCA [13] revealed a prevalence of 36%, 24% and 40% for Type I, II and III respectively.

2.4 Idealized Virtual Doppler Ultrasound

Most studies measuring WSS from V_{max} have employed a small Doppler sample volume placed in the centre of the vessel [1, 7-9]. Alternatively, the sample volume may be positioned at the perceived location of highest velocity ('max-line' velocity), then for the purposes of calculation, assumed to lie on the centreline [11]; the latter approach may be preferable in the presence of

significant velocity profile skewing [16]. To perform an idealized virtual Doppler ultrasound on the 2D velocity profile data, we therefore placed 1.5×1.5 mm square sample volumes 1) in the centre of the lumen or 2) centred at the location of peak maximal velocity (Fig. 1). The virtual Doppler acquisition involved extracting the highest velocity from within the sample volume.

2.5 Wall Shear Stress Calculation

WSS was calculated from V_{max} taken from the respective sample volumes by assuming Poiseuille or Womersley velocity profiles (see Appendix). This approach assumes axisymmetry, and hence that WSS is uniform circumferentially. However, this is not true of the CFD-derived WSS, and therefore reference WSS values were obtained by first extracting values from the CCA wall in 1.5 mm thick slices centered at the chosen slice location (Fig. 2). Since the surface nodes were randomly (albeit evenly) distributed with respect to the circumferential direction, nodal WSS values were interpolated onto a structured grid composed of axial lines (ten nodes each), spaced five degrees apart around the CCA circumference (Fig. 2). WSS was then averaged over each axial line to provide a WSS vector for each of the 72 circumferential sectors, the axial component of which was used for comparison with the V_{max} method. Fig. 3 shows cycle-averaged WSS vectors and associated velocity profiles and HVR in representative cases (all profiles are shown in [16]). Finally, a spatially-averaged WSS waveform was calculated for comparison with the V_{max} method, with specific investigation of cycle-averaged and peak wall shear stress (WSS_{av}, WSS_{peak}). Note that in this study, CFD-derived WSS constitutes the reference point and is referred to as the 'actual' (i.e. true) values; by this we do not imply that CFD-derived values are necessarily identical with in-vivo values. That CFD WSS values may not be 'patient-specific' is therefore not germane to our study.

3. Results

Fig. 4 shows scatterplots of estimated (i.e. Poiseuille/Womersley-derived) WSS for the max-line and centreline sample volumes versus actual (i.e. CFD-derived) values. For WSS_{av} (Fig. 4A), in

which Poiseuille and Womersley approaches are identical, both centreline and max-line sample volumes exhibited substantial spread of the data points about the line of unity. Cases with Type I and Type II cycle-averaged velocity profiles (low/moderate skewing) displayed errors generally within ±25%, although in one case WSS_{av} was overestimated by ~70% (Fig. 4A). For Type III profiles (severe skewing), WSS_{av} was always underestimated, with median and maximum errors of –30% and –55% respectively (Fig. 4A). The difference in percent errors between Type I/II and Type III could not be explained by a proportionality between absolute values and errors, as there was no difference in absolute values between the three groups (as tested with ANOVA). Use of a max-line sample volume produced only a minor reduction (of < 5%) in median errors compared with the centreline sample volume.

When employing a Poiseuille profile, WSS_{peak} was always underestimated, and regardless of the profile type or choice of sample volume, the median error was approximately –50%, while the spread of errors spanned –20% to –65% (Fig. 3B and Fig. 4, right panel). Although median errors were close to zero when assuming a Womersley profile, the range of errors was still ±30% regardless of velocity profile classification.

Representative WSS waveforms are shown in Fig. 6. In all cases, the parabolic profile (dashed blue lines) was clearly unsuitable for estimating pulsatile aspects of WSS (such as WSS_{peak}). In several cases, WSS was relatively well approximated by the Womersley assumption (red lines) over the whole cardiac cycle, as might be expected for Type I (and possibly Type II) velocity profiles (Fig. 5A&D). However, these instances were starkly contrasted by Cases B&E in which WSS ranged circumferentially by up to 50 dynes/cm^2 (i.e. almost 100% of peak WSS) despite being classified as Type I & II respectively. In a number of instances, the Womersley approach did not reveal periods of very low or negative actual WSS (e.g. Fig. 5B&F). Regardless of cycle-averaged profile type, substantial circumferential variation commonly occurred during mid-late systole, coinciding with the most severe velocity profile skewing and consequent underestimation of WSS when averaged over the cardiac cycle (Fig. 5). In Cases G and I, use of

a max-line sample volume only slightly ameliorated the late systolic WSS underestimation compared with the centreline sample volume.

4. Discussion

The assumptions involved in estimating WSS via Doppler V_{max} are well documented, but the nature and degree of errors introduced by them is less appreciated. Flow in the CCA and other nominally 'straight' arteries is generally assumed to be fully-developed and axisymmetric, justifying the use of parabolic or Womersley profiles to derive WSS. However, fully-developed axisymmetric flow is probably the exception rather than the rule even in slightly/locally curved vessels, such as the CCA [13, 14]. Results of the present study, which investigated realistic CCA geometries using CFD, suggest that velocity profile skewing is likely to cause substantial and variable (i.e. wide-ranging and case-dependent) errors in WSS_{av} and WSS_{peak} when estimated from Doppler V_{max}. Moreover, potentially large circumferential WSS variations related to the profile skewing obviously cannot be detected via the V_{max} technique.

4.1 Cycle-averaged wall shear stress (WSS_{av})

To date, the literature has not provided a clear message regarding the degree of error involved in estimating WSS_{av} via Poiseuille's law (note that Womersley's theory is identical for WSS_{av}, so we here refer only to Poiseuille). In an MRI study by Sui et al [20], the Poiseuille approach led to slightly (~10%) higher WSS_{av} values compared with a 3D paraboloid-fitting method, explained on the basis that the Poiseuille method neglects diameter variations during the cardiac cycle. Augst et al [21] reported Poiseuille-derived WSS_{av} as being more than twice that calculated from a CFD model. That result, however, may not be reliable, since the Poiseuille-based WSS was calculated using the diameter of the CFD model inlet, which was less than that at the site of CFD WSS calculation (personal communication with the authors of [21]); noting that, for a fixed flow rate, WSS scales with the inverse cube of diameter, the difference in WSS could be explained if the diameter of the two sites differed by only 20%. Consistent with our results for highly

skewed, or Type III, profiles (Fig. 5, bottom left panel), Dammers et al [22] derived a CCA WSS_{av} of 5.7 dynes/cm^2 via Poiseuille's law, but a value of 11.5 dynes/cm^2 by measuring peak dV/dr near the vessel wall using high resolution multi-gate Doppler ultrasound. Interestingly, the same study reported good agreement in the brachial artery (4.2 vs 4.8 dynes/cm^2), which on the basis of our results, may have occurred due to the velocity profiles being more fully-developed/axisymmetric (i.e. Type I or II, see Fig. 5 top/middle left panels); however, this may not always be the case in the brachial artery [23, 24].

Following previous studies from our laboratory [13, 16], we grouped velocity profiles into axisymmetric (Type I), mildly skewed (Type II) or highly skewed (Type III) classifications, under the hypothesis that greater skewing would be associated with greater WSS errors. For both Type I and Type II profiles, WSS_{av} was underestimated in some cases and overestimated in other cases (i.e. no predictable bias) despite only mild skewing. By contrast, in Type III cases WSS_{av} was consistently underestimated, with a median error of 30%, although the range of errors remained large (i.e. 5% to 55%). Importantly, it was the mid-late systolic period, when the instantaneous velocity profile was most highly skewed [13, 16, 20], that contributed most to the underestimation of WSS_{av} (Fig. 6G-I).

Of particular interest was the finding that even Type I profiles did not 'obey' Poiseuille's law particularly well, with WSS_{av} errors in the range ±25% (Fig. 5). Several factors are likely to contribute to these errors. First, the Type I profiles were not perfectly axisymmetric. Second, even if perfectly axisymmetric, arbitrarily large errors are possible when incorrectly assuming a fully-developed profile. Third, half of the Type I cases (classified on the basis of cycle-averaged velocity profiles) displayed Type III profiles during mid-late systole (e.g. Fig. 6C), consistent with [13]. Finally, because the vessel is not a perfect cylinder, even a relatively axisymmetric and near-fully-developed profile can be associated with substantial circumferential variation in WSS (e.g. Figure 6B), which is likely to translate to errors in WSS_{av}.

4.2 Peak wall shear stress (WSS_{peak})

Numerous studies have reported WSS_{peak} values derived from an assumed Poiseuille velocity profile [1, 2, 7, 8, 25]. To our knowledge, our study is the first to compare WSS_{peak} derived from this commonly-employed technique against its known reference value. Womersley's theory for pulsatile flow predicts a more blunted velocity profile compared with the parabolic profile, and one would therefore expect Poiseuille-derived WSS_{peak} to be underestimated. This is indeed what we observed; regardless of velocity profile classification, Poiseuille-derived WSS_{peak} was underestimated by ~50%. Conversely, no bias was apparent when assuming a Womersley profile, although the range of WSS_{peak} errors was not negligible (±30%).

Consistent with our findings (Fig. 4B), in studies of normal subjects, Stroev et al [12] and Blake et al [26] derived CCA peak wall shear rates of 1640 s^{-1} and 1191 s^{-1} respectively using a Womersley profile, corresponding to WSS_{peak} values of 57 and 42 dynes/cm^2 (assuming a blood viscosity of 0.035 Poise), whereas reported WSS_{peak} values calculated via a parabolic profile have been typically between 20 and 30 dynes/cm^2 [2, 7]. Although studies measuring near-wall velocities using MRI or Doppler have also found WSS_{peak} values between 20 and 30 dynes/cm^2 [20, 27, 28], Oyre et al [27] reported that the V_{max}-Poiseuille approach underestimated WSS_{peak} compared with the near-wall measurement (17 vs 26 dynes/cm^2).

4.3 Circumferential WSS variations

An important consequence of velocity profile skewing is that WSS is likely to vary circumferentially around the vessel wall, being higher near regions of high velocity. At least two MRI studies have found large circumferential WSS variations in the CCA of normal subjects. In Figure 3 of Gelfand et al [29], WSS_{av} was shown to vary between approximately 5 and 25 dynes/cm^2, and WSS_{peak} between 20 and 75 dynes/cm^2; similarly, Figure 8 of Carvalho et al [30] shows instantaneous systolic wall shear rate ranging from approximately 700 to 1800 s^{-1} around the CCA circumference, i.e. WSS between 25 and 63 dynes/cm^2.

Both studies were entirely consistent with our CFD results. On average, WSS_{av} varied circumferentially by ±60% about the circumferential mean (absolute variation 18±11 dynes/cm^2), and in some cases by up to ±100%. Percent variations were lower at peak systole ('P1' in Fig. 6A), averaging ±30% and up to ±70%, although the absolute variation was greater (28±18 dynes/cm^2). Percent variations were highest at the time of the second systolic flow peak ('P2' in Fig. 6A), averaging ±75% (absolute variation 44±19 dynes/cm^2) and as high as ±140%. There was no significant difference in percent variations between Type I, II and III cases, apparently due to our finding that substantial circumferential WSS variations may exist even when the velocity profile is relatively axisymmetric, as for example, in Fig. 6B. In that instance, the sustained circumferential variation was attributed to a slight local narrowing of the vessel upstream to the analysed 2D slice, which caused some flow separation and hence low WSS. In other cases, although the cycle-averaged velocity profile was Type I, a high degree of skewing and circumferential WSS variation occurred during late systole (e.g. Fig. 6C).

4.4 Other methods of calculating WSS

We previously reported that for severe velocity profile skewing, V_{max} may lie outside of a centrally-located sample volume and therefore be underestimated by up to 12% (cycle-averaged) or 27% (maximum instantaneous) [16]. Although this has an appreciable effect when estimating flow variables [16], the current study suggests this phenomenon has little bearing on WSS errors, which are instead dominated by the assumption of fully-developed velocity profile shape. Hence, use of a max-line (rather than centreline) sample volume appears unlikely to substantially improve WSS errors.

Aside from the V_{max}-based methods investigated in the current study, a number of other methods have been proposed for *in vivo* WSS measurement, most of which attempt to measure near-wall velocities and their gradients. Numerous MRI methods have been proposed and we refer to Petersson et al [5] for details. Measuring near-wall velocities with commercial Doppler

ultrasound is very challenging and subject to error [31, 32]. Hence, specialised multi-gate Doppler systems have been designed to optimise the near-wall measurements [33, 34] or to improve assessment of skewed velocity profiles [35]; however these state-of-the-art systems are not widely available. We thus focused our study on the V_{max} techniques that are frequently adopted in clinical studies [1, 2, 7-11].

4.5 Assumptions of Idealised Virtual Doppler Ultrasound and CFD

The virtual Doppler ultrasound applied to CFD data in this study was purposely idealised so that we could assess the likely 'best case' accuracy of WSS measurements given a 'perfect' acquisition. However, besides the fundamental limitation of assuming axisymmetric fully developed flow, several other sources of error are likely to exist in practice. For instance, intrinsic spectral broadening is known to cause 30-50% overestimation of V_{max} [26] and to our knowledge this is not routinely corrected for; based on our results, overestimation of V_{max} may actually offset the underestimation of WSS_{peak} (when calculated via a parabolic profile) or WSS_{av} (for Type III profiles, Fig. 5), but may also cause overestimation of these quantities (when using a Womersley profile or for Type I or II profiles).

We also did not simulate the practical effects of Doppler beam angle and its correction. Since angle correction is performed under the assumption that velocity vectors point in the axial direction only, the presence of secondary flow (i.e. radial and/or circumferential velocity components) may confound measurement of axial velocity [36] and thereby contribute positive or negative bias in calculated WSS. Another consequence of secondary flow is that the WSS vectors may contain in-plane components (Fig. 6, particularly panels E and H, for example), in which case the absolute WSS would be slightly greater than the axial component. Results presented in this paper were calculated from the axial component, as Poiseuille and Womersley approaches assume axial flow; however, all results were essentially identical when calculated

from the WSS vector magnitude, suggesting that the effect of non-axial components was negligible, consistent with [36].

Finally, in our CFD models we assumed the same nominal value of blood viscosity for all subjects, and did not account of the compliance of the CCA. This would not have affected our conclusions, however, given that the comparison between CFD data and the virtual Doppler calculations was internally consistent. Note that, for in-vivo measurements, neglecting diameter variations may contribute significantly to WSS errors. Finally, the impact of assuming a nominal viscosity appears to be minor [37] and hence the results of our study apply equally to the assessment of wall shear rate and wall shear stress.

4.6 Relevance and Perspectives

In a review of WSS measurement, Katritsis et al [38] stated that "[the assumptions required] all seriously limit the application of Poiseuille's law and, thus, limit accordingly the accuracy of WSS estimation by means of the Hagen-Poiseuille formula." However in the same review, it was also stated that "nonetheless, one may accept these assumptions to obtain possibly useful approximations of WSS based on measurements in a clinical context". Herein is the key issue, for even if WSS estimates are subject to error, this does not exclude the measurement from having possible clinical value; after all, it may be argued that every *in vivo* measurement involves assumptions and errors. Whether this is true depends largely on the nature of the errors. If the error produces a predictable bias, the trends may be useful even if the absolute values are wrong. However, if the scatter in the error is large (i.e. comparable to the absolute values), the measurement becomes less useful. In this regard, our data provides caution in estimating WSS from V_{max} in two key respects.

First, velocity profile skewing, which is probably common in the CCA [13] and may occur in the brachial and femoral arteries [15, 23, 24], is likely to substantially degrade the accuracy of average or peak WSS measurements. Importantly, we found a large degree of

variability in the errors, which may limit the specificity and sensitivity of clinical studies. As an example, we observed cases in which WSS_{peak} estimated via the Poiseuille approach were all ~20 dynes/cm^2, but the actual values ranged between 28 dynes/cm^2 and 60 dynes/cm^2 (Fig. 4, right panel). Similarly, for WSS_{av}, cases with actual values of 9 or 22 dynes/cm^2 equally had V_{max}-derived values of ~16 dynes/cm^2.

Second, our results highlight that the use of V_{max} to derive a single value for WSS cannot capture possibly large circumferential variation of WSS. If the WSS experienced by endothelial cells differs in some cases by up to ±100% of the circumferentially averaged value, as our data suggests, the physiological significance of the average value may be questioned. For example, in a number of cases (e.g. Fig. 6B&F), local WSS was near-zero or oscillatory at certain times in the cardiac cycle, but this phenomenon was not reflected in the Poiseuille or Womersley-derived WSS waveforms. In other cases (e.g. Fig. 6I), the highest WSS experienced by some parts of the vessel wall was profoundly underestimated.

Finally, as already alluded to, although we did not specifically study the femoral or brachial arteries, the conclusions of our study may also apply to these 'long, straight' vessels in which fully-developed flow is often assumed.

5. Conclusions

Doppler-V_{max} WSS measurement is generally applied to 'sufficiently straight' vessels, justifying the assumption of an axisymmetric fully-developed velocity profile. However, even slight curvatures of nominally 'straight' vessels may lead to significant velocity profile skewing and substantial errors in calculated WSS. Our data suggested that, given an ideal Doppler acquisition, peak systolic WSS may be underestimated by 30-60% when assuming a parabolic velocity profile and ±30% when assuming a Womersley profile, while errors of 20-50% are likely for cycle-averaged WSS, depending on the degree of profile skewing. Finally, the V_{max} technique cannot detect the presence of (possible large) circumferential WSS variations. Since significant

skewing may exist even where there is no local curvature, due to a persistence of skewing arising from upstream curvatures [14], it is difficult to provide anatomically-based guidelines for minimizing WSS measurement errors. Instead, on the basis of our results, we recommend that alternative WSS estimation methods that do not require an assumption of fully-developed axisymmetric velocity profiles, such as high resolution MRI or multi-gate Doppler, be further pursued.

Acknowledgments

This work was supported by grant NA6727 from the Heart & Stroke Foundation of Canada. The VALIDATE study is supported by Contract No. NO1-AG-3-1003 from the National Institute on Aging, NIH and, in part, by the Intramural Research Program of the National Institute on Aging, NIH. JPM was supported by an Overseas Biomedical Training Fellowship from the National Health and Medical Research Council of Australia. DAS was supported by a Heart and Stroke Foundation Career Investigator Award.

Appendix

Wall shear stress (τ) is defined as

$$\tau = \mu \left. \frac{\partial V}{\partial r} \right|_R \tag{1}$$

where μ is the dynamic viscosity, R is the effective vessel radius (i.e. $\sqrt{A/\pi}$, where A is cross-sectional area), and r is the radial coordinate. If a parabolic (Poiseuille) velocity profile is assumed, it can be shown from Equation (1) that

$$\tau_P(t) = \frac{4\mu}{D} V_{max}(t) \tag{2}$$

where D is diameter. Accounting for flow pulsatility via Womersley's theory leads to the following expression,

$$\tau_W(t) = \tau_P(t) + \frac{2\mu}{D} V_{max}(t)\,\mathrm{Re}\left[-\sum_{k=1}^{\infty} \left(\frac{\zeta_k J_1(\zeta_k)}{J_0(\zeta_k) - 1} \right) e^{i\omega_k t} \right] \quad (3)$$

where $\zeta_k = i^{3/2}\alpha_k$, $\alpha_k = R\sqrt{\omega k \rho / \mu}$ is the Womersley number, ρ is blood density, ω is angular frequency, and J_0 and J_1 are first order Bessel functions of the first and second kind.

References

1. Gnasso A, Carallo C, Irace C*, et al*: Association between wall shear stress and flow-mediated vasodilation in healthy men. Atherosclerosis 2001, 156(1):171-176.
2. Gnasso A, Carallo C, Irace C*, et al*: Association Between Intima-Media Thickness and Wall Shear Stress in Common Carotid Arteries in Healthy Male Subjects. Circulation 1996, 94(12):3257-3262.
3. Gnasso A, Irace C, Carallo C*, et al*: In Vivo Association Between Low Wall Shear Stress and Plaque in Subjects With Asymmetrical Carotid Atherosclerosis. Stroke 1997, 28(5):993-998.
4. Malek AM, Alper SL, Izumo S: Hemodynamic Shear Stress and Its Role in Atherosclerosis. JAMA: The Journal of the American Medical Association 1999, 282(21):2035-2042.
5. Petersson S, Dyverfeldt P, Ebbers T: Assessment of the accuracy of MRI wall shear stress estimation using numerical simulations. J Magn Reson Imaging 2012, 36(1):128-138.
6. Cobbold RSC: Foundations of Biomedical Ultrasound. New York: Oxford University Press; 2007.
7. Jiang Y, Kohara K, Hiwada K: Low wall shear stress in carotid arteries in subjects with left ventricular hypertrophy. Am J Hypertens 2000, 13(8):892-898.
8. Irace C, Cortese C, Fiaschi E, Carallo C, Farinaro E, Gnasso A: Wall Shear Stress Is Associated With Intima-Media Thickness and Carotid Atherosclerosis in Subjects at Low Coronary Heart Disease Risk. Stroke 2004, 35(2):464-468.
9. Carallo C, Lucca LF, Ciamei M, Tucci S, de Franceschi MS: Wall shear stress is lower in the carotid artery responsible for a unilateral ischemic stroke. Atherosclerosis 2006, 185(1):108-113.
10. Parker BA, Ridout SJ, Proctor DN: Age and flow-mediated dilation: a comparison of dilatory responsiveness in the brachial and popliteal arteries. Am J Physiol Heart Circ Physiol 2006, 291(6):H3043-H3049.
11. Simon AC, Levenson J, Flaud P: Pulsatile flow and oscillating wall shear stress in the brachial artery of normotensive and hypertensive subjects. Cardiovasc Res 1990, 24(2):129-136.
12. Stroev PV, Hoskins PR, Easson WJ: Distribution of wall shear rate throughout the arterial tree: A case study. Atherosclerosis 2007, 191(2):276-280.
13. Ford MD, Xie YJ, Wasserman BA, Steinman DA: Is flow in the common carotid artery fully developed? Physiol Meas 2008, 29(11):1335-1349.
14. Manbachi A, Hoi Y, Wasserman BA, Lakatta EG, Steinman DA: On the shape of the common carotid artery with implications for blood velocity profiles. Physiol Meas 2011, 32(12):1885-1897.
15. Wood NB, Zhao SZ, Zambanini A*, et al*: Curvature and tortuosity of the superficial femoral artery: a possible risk factor for peripheral arterial disease. J Appl Physiol 2006, 101(5):1412-1418.
16. Mynard JP, Steinman DA: Effect of velocity profile skewing on blood velocity and volume flow waveforms derived from maximum Doppler spectral velocity. Ultrasound Med Biol, In Press.
17. Ferrucci L: The Baltimore Longitudinal Study of Aging (BLSA): A 50-Year-Long Journey and Plans for the Future. J Gerontol A Biol Sci Med Sci 2008, 63(12):1416-1419.

18. Hoi Y, Wasserman BA, Lakatta EG, Steinman DA: Effect of Common Carotid Artery Inlet Length on Normal Carotid Bifurcation Hemodynamics. J Biomech Eng 2010, 132(12):121008.
19. Moyle KR, Antiga L, Steinman DA: Inlet conditions for image-based CFD models of the carotid bifurcation: Is it reasonable to assume fully developed flow? J Biomech Eng 2006, 128(3):371.
20. Sui B, Gao P, Lin Y, Gao B, Liu L, An J: Assessment of Wall Shear Stress in the Common Carotid Artery of Healthy Subjects Using 3.0-Tesla Magnetic Resonance. Acta Radiol 2008, 49(4):442-449.
21. Augst AD, Ariff B, McG. Thom SAG, Xu XY, Hughes AD: Analysis of complex flow and the relationship between blood pressure, wall shear stress, and intima-media thickness in the human carotid artery. Am J Physiol Heart Circ Physiol 2007, 293(2):H1031-H1037.
22. Dammers R, Stifft F, Tordoir JHM, Hameleers JMM, Hoeks APG, Kitslaar PJEHM: Shear stress depends on vascular territory: comparison between common carotid and brachial artery. J Appl Physiol 2003, 94(2):485-489.
23. Leguy CAD, Bosboom EMH, Hoeks APG, van de Vosse FN: Assessment of blood volume flow in slightly curved arteries from a single velocity profile. J Biomech 2009, 42(11):1664-1672.
24. Silber HA, Ouyang P, Bluemke DA, Gupta SN, Foo TK, Lima JAC: Why is flow-mediated dilation dependent on arterial size? Assessment of the shear stimulus using phase-contrast magnetic resonance imaging. Am J Physiol Heart Circ Physiol 2005, 288(2):H822-H828.
25. Cebral JR, Castro MA, Putman CM, Alperin N: Flow–area relationship in internal carotid and vertebral arteries. Physiol Meas 2008, 29(5):585.
26. Blake JR, Meagher S, Fraser KH, Easson WJ, Hoskins PR: A Method to Estimate Wall Shear Rate with a Clinical Ultrasound Scanner. Ultrasound Med Biol 2008, 34(5):760-774.
27. Oyre S, Ringgaard S, Kozerke S*, et al*: Accurate noninvasive quantitation of blood flow, cross-sectional lumen vessel area and wall shear stress by three-dimensional paraboloid modeling of magnetic resonance imaging velocity data. J Am Coll Cardiol 1998, 32(1):128-134.
28. Kornet L, Lambregts J, Hoeks APG, Reneman RS: Differences in Near-Wall Shear Rate in the Carotid Artery Within Subjects Are Associated With Different Intima-Media Thicknesses. Arterioscler Thromb Vasc Biol 1998, 18(12):1877-1884.
29. Gelfand BD, Epstein FH, Blackman BR: Spatial and spectral heterogeneity of time-varying shear stress profiles in the carotid bifurcation by phase-contrast MRI. J Magn Reson Imaging 2006, 24(6):1386-1392.
30. Carvalho JLA, Nielsen J-F, Nayak KS: Feasibility of in vivo measurement of carotid wall shear rate using spiral fourier velocity encoded MRI. Magn Reson Med 2010, 63(6):1537-1547.
31. Leguy C, Bosboom E, Hoeks A, van de Vosse F: Model-based assessment of dynamic arterial blood volume flow from ultrasound measurements. Med Biol Eng Comput 2009, 47(6):641-648.
32. Gijsen FJH, Brands PJ, Van de Vosse FN, J.D. J: Assessment of wall shear rate measurements with ultrasound. Journal of Vascular Investigation 1998, 4(4):187-197.
33. Brands PJ, Hoeks APG, Hofstra L, Reneman RS: A noninvasive method to estimate wall shear rate using ultrasound. Ultrasound Med Biol 1995, 21(2):171-185.
34. Tortoli P, Morganti T, Bambi G, Palombo C, Ramnarine KV: Noninvasive simultaneous assessment of wall shear rate and wall distension in carotid arteries. Ultrasound Med Biol 2006, 32(11):1661-1670.

35. Beulen B, Verkaik A, Bijnens N, Rutten M, van de Vosse F: Perpendicular ultrasound velocity measurement by 2D cross correlation of RF data. Part B: volume flow estimation in curved vessels. Experiments in Fluids 2010, 49(6):1219-1229.
36. Krams R, Bambi G, Guidi F, Helderman F, van der Steen AF, Tortoli P: Effect of vessel curvature on Doppler derived velocity profiles and fluid flow. Ultrasound Med Biol 2005, 31(5):663-671.
37. Parkhurst KL, Lin H-F, DeVan AE, Barnes JN, Tarumi T, Tanaka H: Contribution of blood viscosity in the assessment of flow-mediated dilation and arterial stiffness. Vasc Med 2012, 17(4):231-234.
38. Katritsis D, Kaiktsis L, Chaniotis A, Pantos J, Efstathopoulos EP, Marmarelis V: Wall Shear Stress: Theoretical Considerations and Methods of Measurement. Prog Cardiovasc Dis 2007, 49(5):307-329.

Fig. 1. Illustration of the idealised sample volumes (centreline, max-line) in the virtual Doppler ultrasound, shown in relation to the three velocity profile classifications: axisymmetric (Type I), skewed (Type II) and crescent (Type III).

Fig. 2. Wall shear stress (WSS) was extracted from the common carotid artery (CCA) of CFD models by defining 1.5 mm wide bands centred at approximately 1, 3 and 5 cm from the bifurcation apex and interpolating calculated WSS from the CFD surface mesh onto axial lines spaced 5º apart circumferentially (red dots). WSS at a given circumferential location was obtained by averaging over the corresponding axial line. ECA, external carotid artery; ICA, internal carotid artery.

Fig. 3. Representative cycle-averaged velocity profiles and wall shear stress vectors from the CFD models of the common carotid artery. The white contour corresponds to the 'high velocity region' used to classify the profile type.

Fig. 4. (A) Cycle-averaged wall shear stress (WSS_{av}) and (B) peak wall shear stress (WSS_{peak}) versus values estimated via assumed Poiseuille or Womersley velocity profiles, calculated from V_{max} obtained with a centreline or max-line sample volume. Note that WSS_{av} is identical for Poiseuille and Womersley profiles. Data are grouped by cycle-averaged velocity profile classification: Type I (axisymmetric), Type II (skewed) and Type III (crescent).

Fig. 5. Percentage errors in cycle-averaged wall shear stress (WSS_{av}) and peak wall shear stress (WSS_{peak}) when calculated from the virtual Doppler ultrasound using max-line (ML) or centreline (CL) sample volumes, and by assuming Poiseuille or Womersley flow conditions. Red bars indicate median errors, circles represent individual data points and a negative error corresponds to underestimation.

Fig. 6. Wall shear stress (WSS) waveforms derived via Poiseuille (dashed blue lines) and Womersley (solid red lines) using the centreline sample volume. Actual wall shear stress is shown as a grey scale distribution, with a black line indicating the median instantaneous WSS of all circumferential values, while the faintest shades of grey reach to the maximum and minimum

WSS values. Note that for cases G and I, waveforms for the max-line sample volume are shown using thin red and dashed blue lines; in all other cases these were negligibly different from the centreline waveforms and are not shown. Velocity scale range is maximized in each contour plot (as in Fig. 3). Instantaneous velocity profiles at peak systole (P1) and the second systolic peak (P2), along with corresponding WSS vectors, are inset on each panel, with arrows showing the time of P1 and P2. Colour in online version only.

Fig. 1. Illustration of the idealised sample volumes (centreline, max-line) in the virtual Doppler ultrasound, shown in relation to the three velocity profile classifications: axisymmetric (Type I), skewed (Type II) and crescent (Type III).

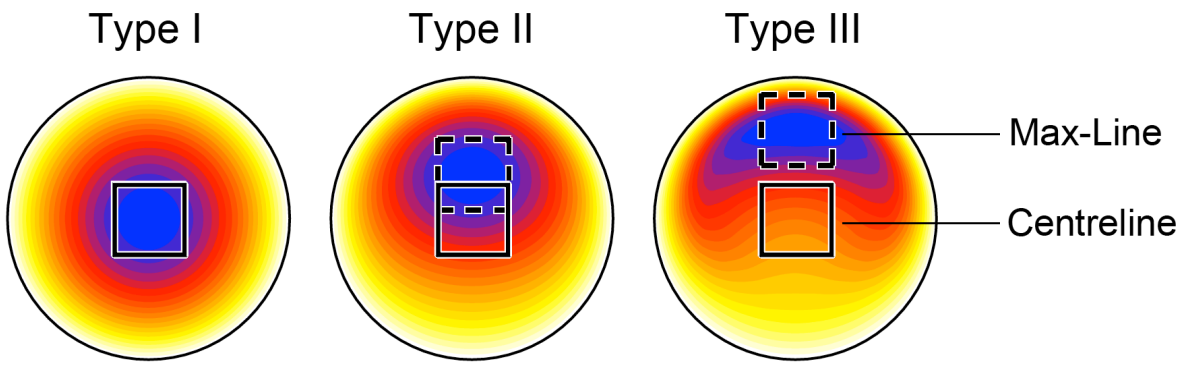

Fig. 2. Wall shear stress (WSS) was extracted from the common carotid artery (CCA) of CFD models by defining 1.5 mm wide bands centred at approximately 1, 3 and 5 cm from the bifurcation apex and interpolating calculated WSS from the CFD surface mesh onto axial lines spaced 5º apart circumferentially (red dots). WSS at a given circumferential location was obtained by averaging over the corresponding axial line. ECA, external carotid artery; ICA, internal carotid artery.

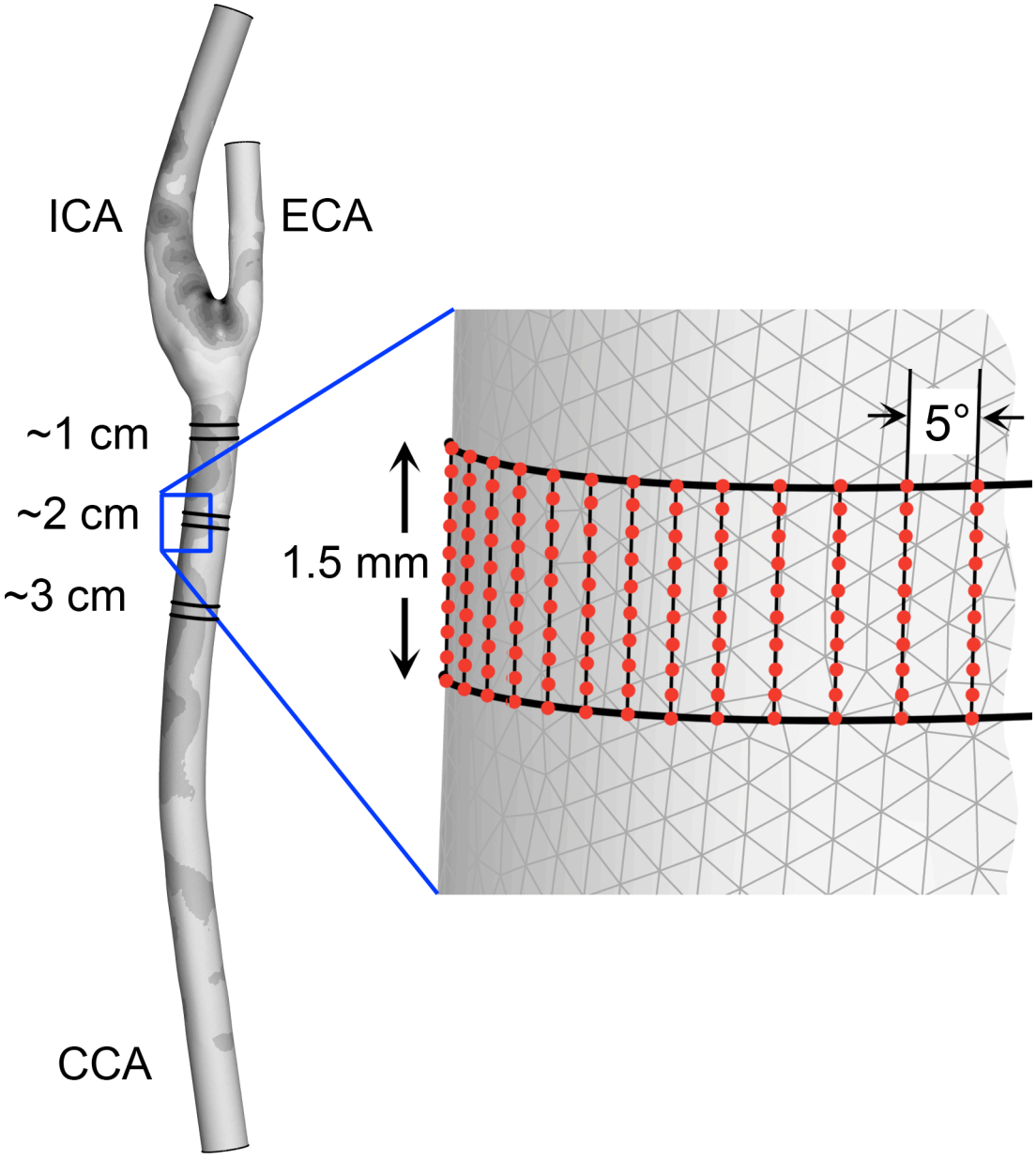

Fig. 3. Representative cycle-averaged velocity profiles and wall shear stress vectors from the CFD models of the common carotid artery. The white contour corresponds to the 'high velocity region' used to classify the profile type.

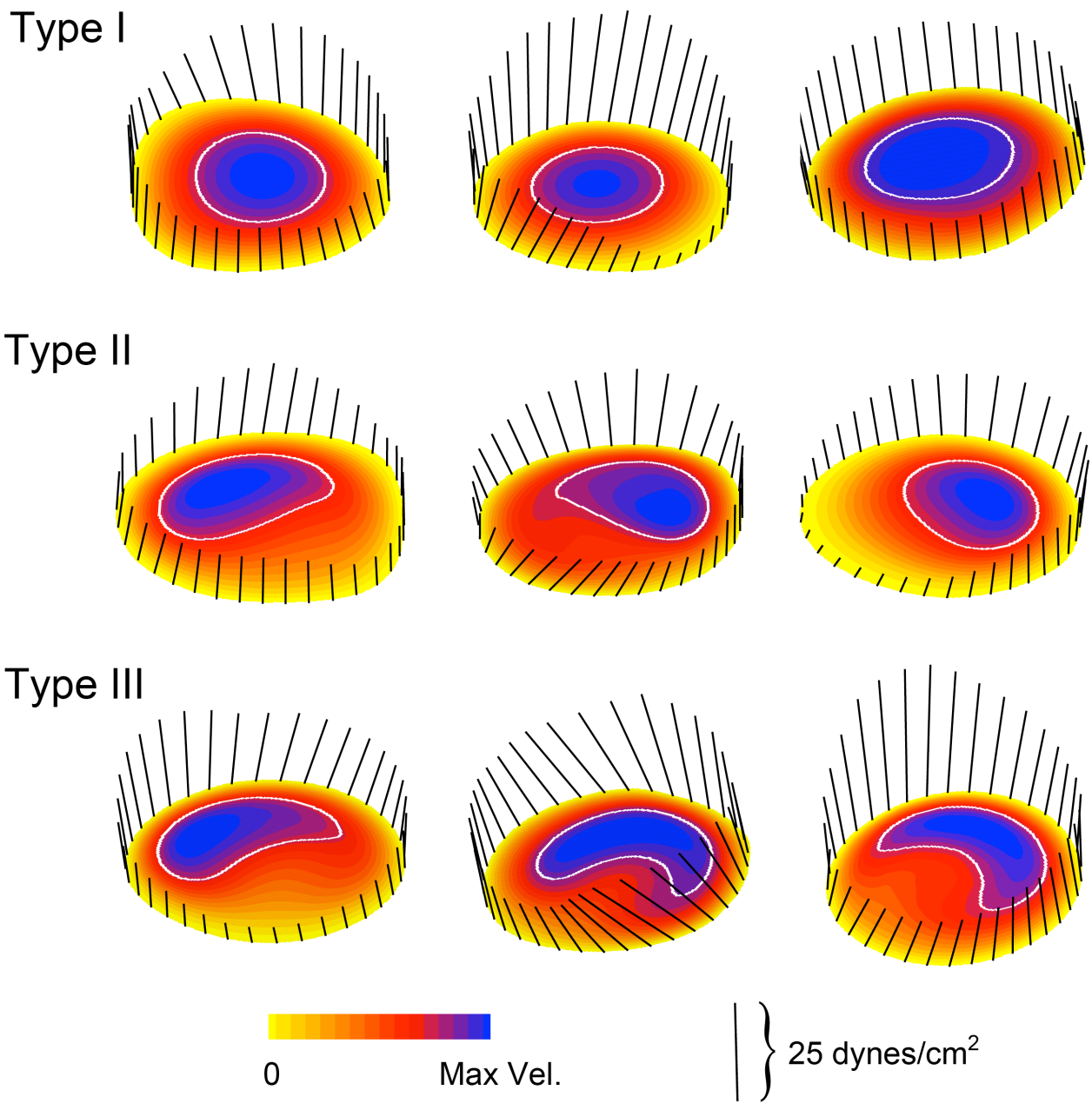

Fig. 4. (A) Cycle-averaged wall shear stress (WSS_{av}) and (B) peak wall shear stress (WSS_{peak}) versus values estimated via assumed Poiseuille or Womersley velocity profiles, calculated from V_{max} obtained with a centreline or max-line sample volume. Note that WSS_{av} is identical for Poiseuille and Womersley profiles. Data are grouped by cycle-averaged velocity profile classification: Type I (axisymmetric), Type II (skewed) and Type III (crescent).

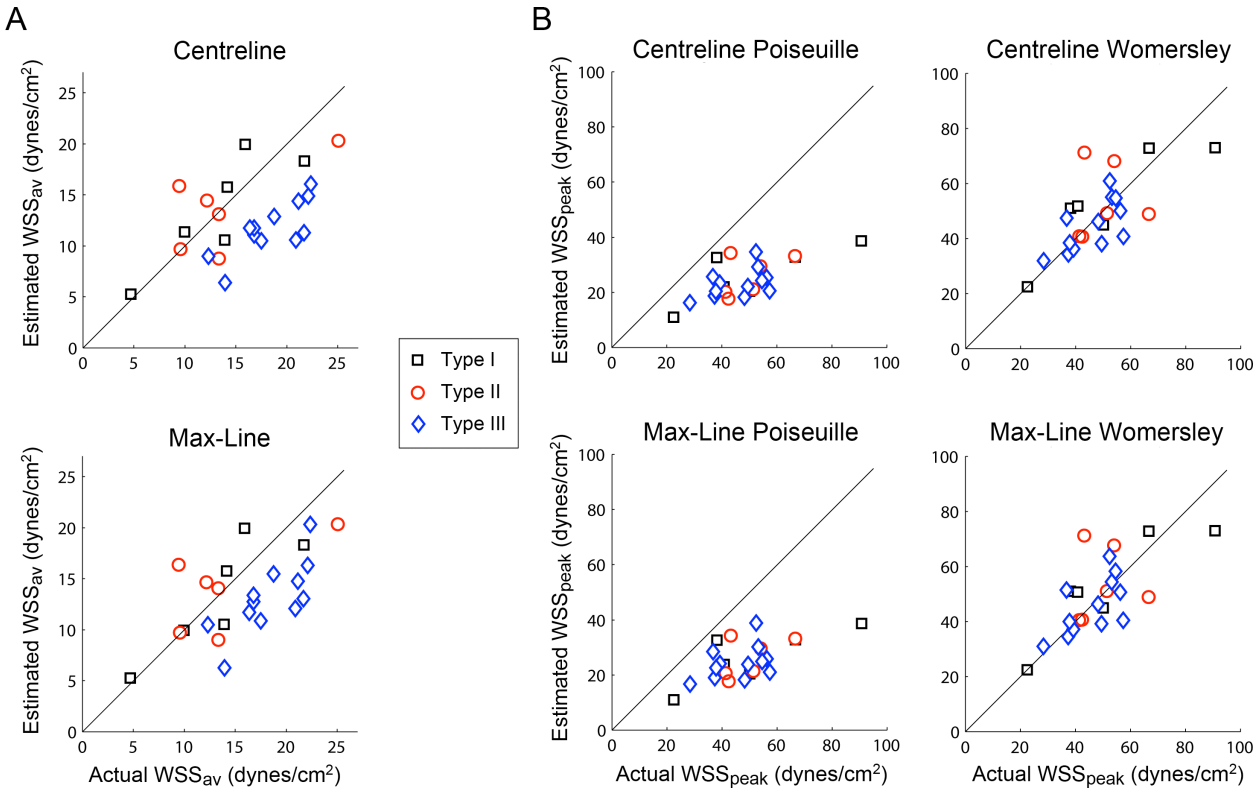

Fig. 5. Percentage errors in cycle-averaged wall shear stress (WSS_{av}) and peak wall shear stress (WSS_{peak}) when calculated from the virtual Doppler ultrasound using max-line (ML) or centreline (CL) sample volumes, and by assuming Poiseuille or Womersley flow conditions. Red bars indicate median errors, circles represent individual data points and a negative error corresponds to underestimation.

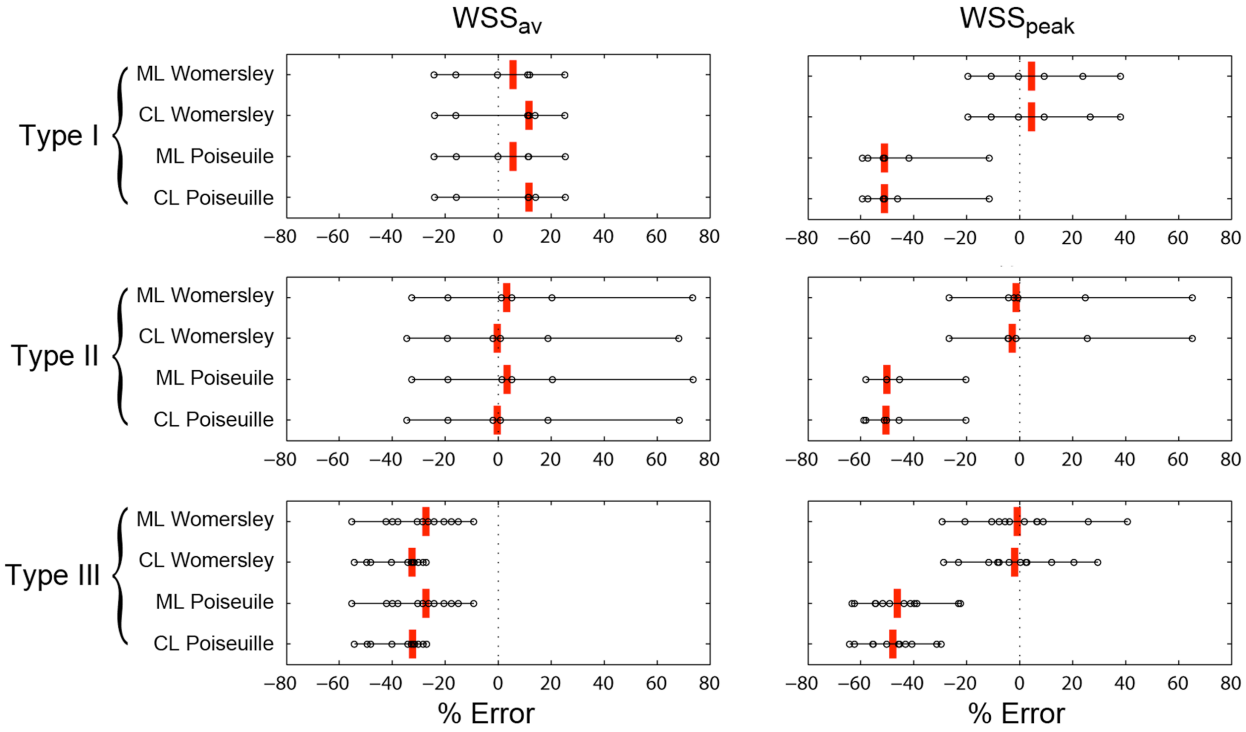

Fig. 6. Wall shear stress (WSS) waveforms derived via Poiseuille (dashed blue lines) and Womersley (solid red lines) using the centreline sample volume. Actual wall shear stress is shown as a grey scale distribution, with a black line indicating the median instantaneous WSS of all circumferential values, while the faintest shades of grey reach to the maximum and minimum WSS values. Note that for cases G and I, waveforms for the max-line sample volume are shown using thin red and dashed blue lines; in all other cases these were negligibly different from the centreline waveforms and are not shown. Velocity scale range is maximized in each contour plot (as in Fig. 3). Instantaneous velocity profiles at peak systole (P1) and the second systolic peak (P2), along with corresponding WSS vectors, are inset on each panel, with arrows showing the time of P1 and P2. Colour in online version only.